ELSEVIER

Journal of Constructional Steel Research 57 (2001) 45–70

JOURNAL OF CONSTRUCTIONAL STEEL RESEARCH

www.elsevier.com/locate/jcsr

A ductility model for steel connections

L. Simões da Silva [a,*], Ana Girão Coelho [b]

[a] *Departamento de Engenharia Civil, Universidade de Coimbra, Polo II, Pinhal de Marrocos, 3030-290 Coimbra, Portugal*

[b] *Departamento de Engenharia Civil, Instituto Superior de Engenharia de Coimbra, Quinta da Nora, Apartado 10057, 3031-601 Coimbra, Portugal*

Received 28 June 1999; received in revised form 29 November 1999; accepted 23 February 2000

Abstract

A model for the evaluation of the ductility of steel connections loaded in bending is presented in this paper. In the context of the component method, whereby a joint is modelled as an assembly of springs (components) and rigid links, using an elastic post-buckling analogy to the bi-linear elastic–plastic behaviour of each component, a general analytical model is proposed that yields the maximum rotation of the connection. Despite the complexity of the various connection types, the proposed model is able to provide analytical solutions for the moment–rotation response of a steel connection by using appropriate transformation criteria for assemblies of components in series and in parallel. The model is applied to typical beam-to-column connections, showing good agreement with numerical results.

Keywords: Steel; Joints; Bending; Component method; Non-linear behaviour; Ductility

1. Introduction

The evaluation of the ductility of steel and composite connections requires an incremental non-linear analysis. In the context of the component method [1], whereby a joint is modelled as an assembly of springs (components) and rigid links, and concentrating on beam-to-column and beam-to-beam joints, several components contribute to the overall response of the connection, namely: (i) column web in shear, (ii) column web in compression, (iii) column web in tension, (iv) column flange in

* Corresponding author. Tel.: +351 239 797216; fax: +351 239 797217.
E-mail address: luis_silva@gipac.pt (L. Simões da Silva).

0143-974X/01/$ - see front matter
PII: S0143-974X(00)00009-2

Nomenclature

h	Position of the centre of rotation
h_i	Position of component i with respect to the centre of rotation
i	Number of bolt rows; component
k_e	Initial elastic stiffness
k_{ei}	Component i initial elastic stiffness
$k_{e,eq}$	Equivalent elastic stiffness for assemblies of components (series or parallel)
k_p	Post-limit stiffness
k_{pi}	Component i post-limit stiffness
$k_{p,eq}$	Equivalent post-limit for assemblies of components (series or parallel)
$q_{1,\phi}$	Total rotation of the joint
q_2	Rotation of rigid links (compression zone)
q_3	Rotation of rigid links (tension zone)
q_4	Axial displacement of the connection
z	Lever arm
z_i	Distance between the compression member and bolt row i in tension
K	Stiffness (general)
L	Length of rigid links
L_i	Length of rigid links for component i
F	Force
F_c	Axial force (compression zone)
F_t	Axial force (tension zone)
F^C	Strength (limit load)
F_i^C	Component i strength
$M_{j.Rd}$	Flexural resistance
P_i	Critical point
P^B	Twice the limit load
P_{eq}^B	Twice the limit load for equivalent component
P_i^B	Twice the limit load for component i
Q_1	Total displacement (level of applied force)
Q_{1_i}	Displacement of elastic spring i
Q_{2_i}	Rotation of rigid links of length L_i
$S_{j.ini}$	Initial stiffness of the connection
ϵ	Relative error
ϕ_1	Joint rotation when the first component reaches its elastic limit
ϕ_f	Joint rotation at failure
Δ	Total (axial) displacement
Δ_i	Total displacement of component i
$\Delta_{e,i}$	Elastic displacement of component i
$\Delta_{p,i}$	Plastic displacement of component i

Δ^c	Total displacement for the compression zone
Δ^f	Collapse displacement
Δ^t	Total displacement for the tensile zone
Δ^y	Yield displacement
Δ_i^f	Collapse displacement for component *i*
Δ_i^y	Yield displacement for component *i*
Φ_i	Component *i* ductility index
Φ_{joint}	Joint ductility index

bending, (v) end-plate in bending, (vi) flange cleat in bending, (vii) beam flange in compression, (viii) beam web in tension or compression, (ix) plate in tension or compression, (x) bolts in tension, (xi) bolts in shear, (xii) bolts in bearing and (xiii) welds. Each are characterised by a bi-linear force-displacement curve [2], typically represented in Fig. 1, where k_e, k_p, F^C, Δ^y and Δ^f denote, respectively, the initial elastic stiffness, the post-limit stiffness, the strength, the yield displacement and the collapse displacement of the component, P^B being defined as twice the limit load F^C.

Steel joints may present a variety of geometries, with different numbers of bolt rows and connecting parts. Because of this variety of configurations, joint models may range from a simple three-component model as in a welded beam-to-column connection, shown in Fig. 2, to a complex extended end-plate multi bolt-row beam-to-column connection, illustrated in Fig. 3. Despite the differences in these joint models, they share some basic features, namely the subdivision into a tension zone, concentrating all components in tension, a compression zone and a shear zone.

In a recent paper [2], a numerical procedure for the assessment of ductility of steel connections was proposed, which involved the identification of the "yield" sequence of the various components, the definition of a component *i* ductility index, Φ_i and the evaluation of the corresponding joint ductility index, Φ_{joint}, respectively defined by

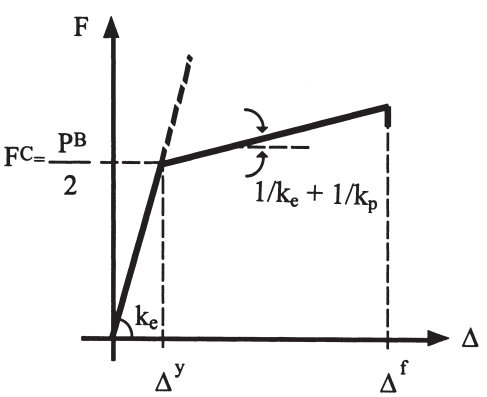

Fig. 1. Typical force-displacement diagram for generic component.

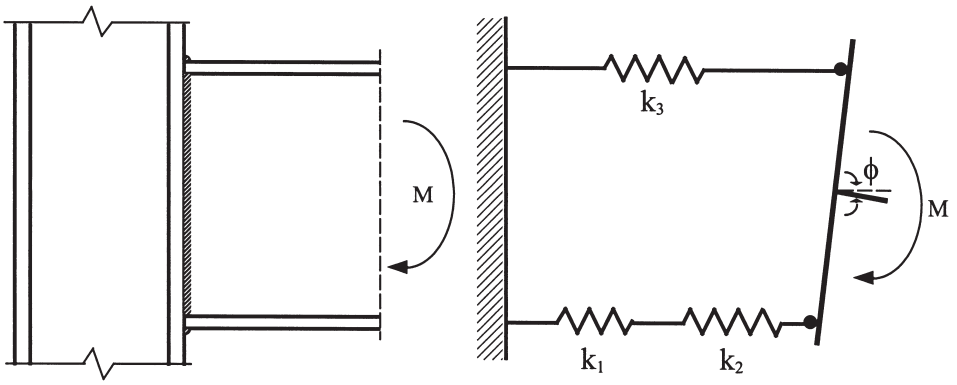

Fig. 2. Mechanical model for welded beam-to-column connection.

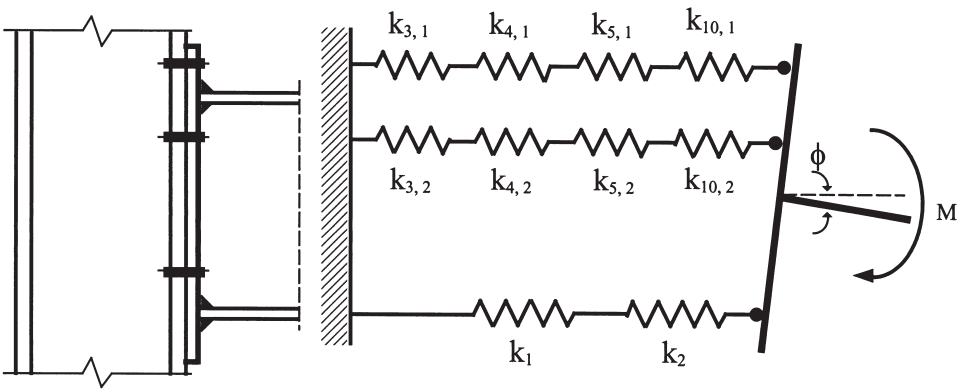

Fig. 3. Mechanical model for extended end-plate beam-to-column connection.

$$\Phi_i=\frac{\Delta_i^{\mathrm{f}}}{\Delta_i^{\mathrm{y}}} \qquad \Phi_{\mathrm{joint}}=\frac{\phi_{\mathrm{f}}}{\phi_1} \tag{1}$$

where ϕ_{f} denotes the joint rotation at failure and ϕ_1 the joint rotation when the first component reaches its elastic limit.

It is the purpose of the present paper to propose a general ductility model for the evaluation of joint behaviour subject to bending.

2. Ductility model

2.1. Introduction

The analysis of connections is currently based on mechanical models of extensional springs and rigid links, as shown in Figs. 2 and 3. Because of the large number

of components that such configurations may present, obtaining analytical solutions requires simplification of the mechanical model. Since all connection models are composed of a tension zone, a compression zone and a shear zone, it is possible to define for any configuration a simple substitute model, consisting of equivalent springs which retain all the original relevant characteristics. This simplified model, illustrated in Fig. 4(b), exhibits the same behaviour as the original one — Fig. 4(a) — and consists of a tension zone and a compression/shear zone. Referring to Fig. 4(b), the lever arm z is defined as the distance between the tension zone and the compression zone, h is defined as the distance between the tension zone and the centre of rotation.

In order to obtain analytical solutions for the complex system from Fig. 4(b), an incremental non-linear procedure is required. Using the approach presented in [3]

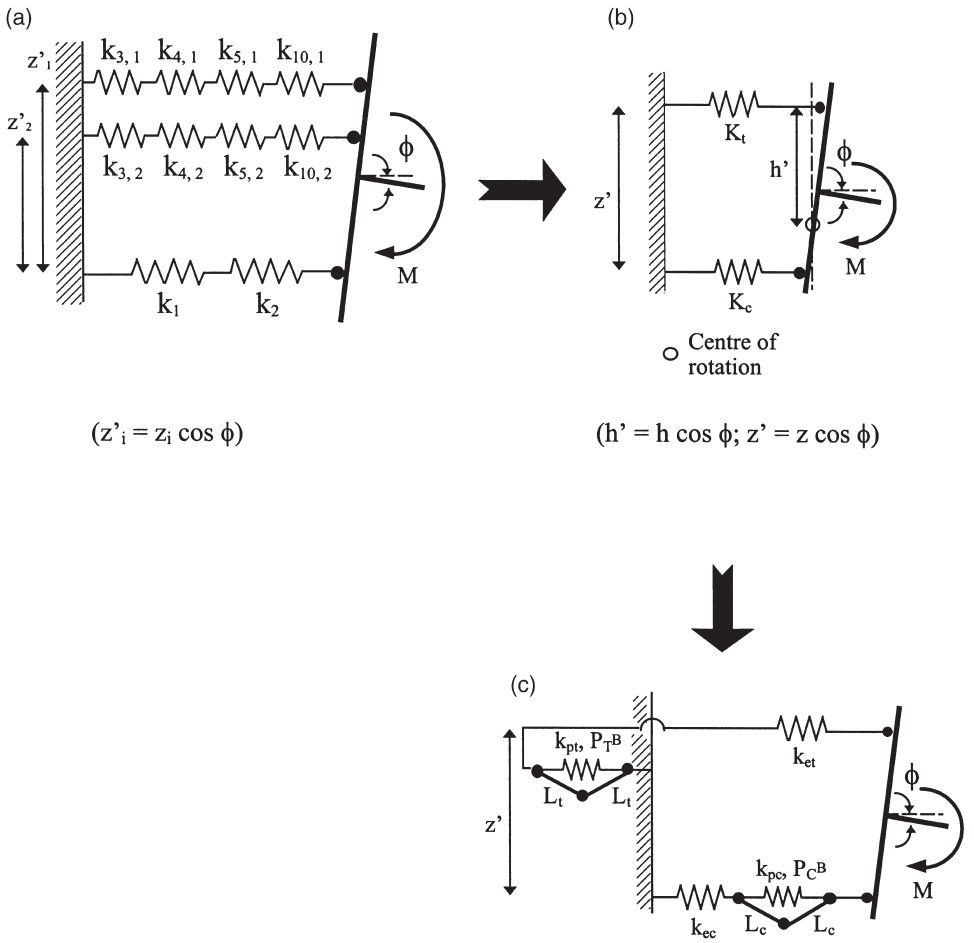

Fig. 4. General substitute model for steel connections. (a) Original model; (b) Equivalent model; (c) Equivalent elastic model.

of the equivalent elastic model of Fig. 4(b), analytical solutions are obtained, reproducing the non-linear moment–rotation response of the connection. The basic building block consists of the two degree-of-freedom system of Fig. 5(a), which consists of one elastic spring with stiffness k_e and a second elastic spring with stiffness k_p and resistance F^C (= $P^B/2$), applied as a pre-compression, the degrees-of-freedom being defined as follows

Q_1 — total displacement;
Q_2 — rotation of rigid links.

Clearly, this model exhibits distinct behaviour in tension and compression, yielding the following equilibrium solutions for compressive and tensile loading, respectively:

$$\begin{cases} F=k_e Q_1 \\ F=\dfrac{k_e}{k_e+k_p}\left(k_p Q_1+\dfrac{P^B}{2}\right) \end{cases} \qquad F=k_e Q_1 \tag{2}$$

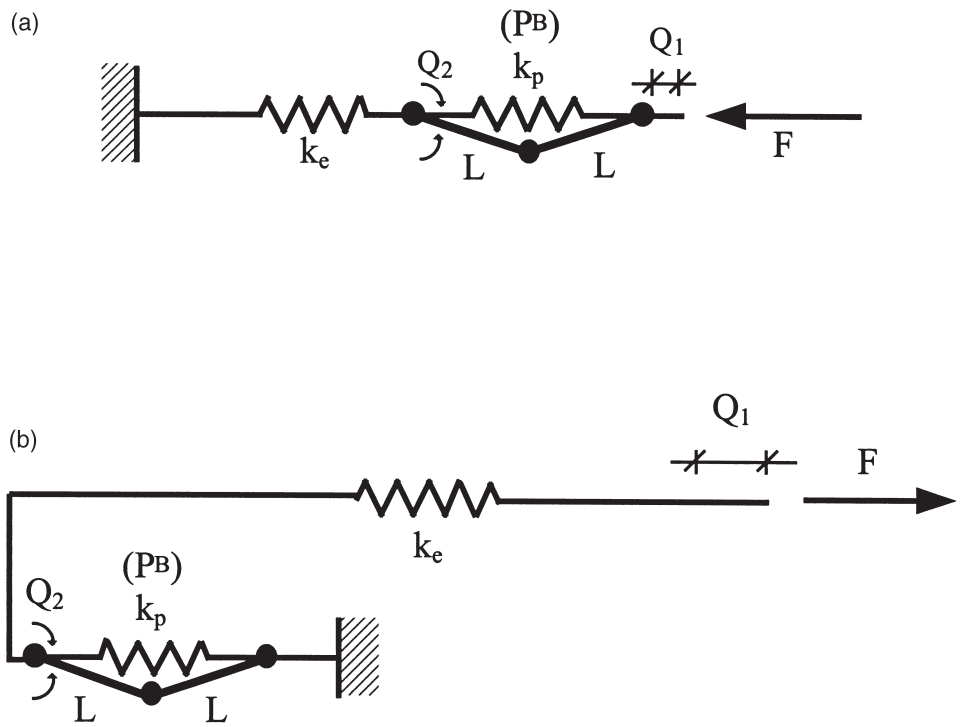

Fig. 5. Equivalent elastic system for elasto-plastic spring. (a) Spring in compression; (b) Spring in tension.

effectively reproducing the original elastic–plastic behaviour of each component. For a component loaded in tension, the equivalent system of Fig. 5(b) yields identical response in tension (bi-linear) and compression (linear).

2.2. Equivalent elastic system for elastic–plastic springs in series

Examination of Fig. 4(a) shows that the tensile or compressive zones of a steel joint often comprise a sequence of components assembled in series. Dealing with the simpler substitute model of Fig. 4(c) requires replacing the real assembly of components in series with a single equivalent spring, as shown in Fig. 6(a). It is thus necessary to define an equivalent elastic system to be able to apply the procedure developed in [4] of replacing each bi-linear spring with an assembly of two elastic springs, as illustrated in Fig. 6(b).

The $2n+1$ degree-of-freedom system of Fig. 6(a) comprises the following degrees-of-freedom

Q_1 — total displacement;
Q_{1_i} — displacement of elastic spring i;
Q_{2_i} — rotation of rigid links of length L_i,

yielding 2^n equilibrium paths. Numbering all components according to increasing limit force F_i^C, the following first $n+1$ equilibrium solutions are obtained, next reproduced with reference to [4]

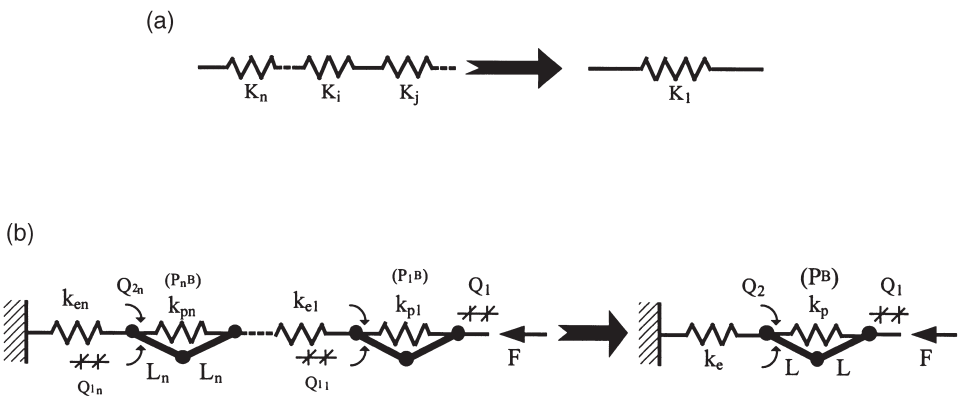

Fig. 6. Equivalent transformation for assembly of components in series. (a) Single equivalent elastic-plastic spring; (b) Equivalent elastic system transformation.

S_1: Fundamental (linear elastic) solution:

$$\begin{cases} Q_{2_1}=0 \\ Q_{2_2}=0 \\ \dots \\ Q_{2_{n-1}}=0 \\ Q_{2_n}=0 \end{cases} \Rightarrow F=\frac{1}{\sum_{i=1}^{n}\frac{1}{k_{ei}}}Q_1 \tag{3}$$

S_j: Equilibrium solution j ($2\le j\le n+1$):

$$F^{(j)}=\frac{1}{\sum_{i=1}^{n}\frac{1}{k_{ei}}+\sum_{i=1}^{j-1}\frac{1}{k_{pi}}}\left(Q_1+\sum_{i=1}^{j-1}\frac{P_i^B}{2k_{pi}}\right) \tag{4}$$

corresponding to the force-displacement diagram of Fig. 7.

Again, following [4], it is thus possible to establish the simpler equivalent elastic system of Fig. 6(b), where $k_{e,eq}$ denotes the equivalent initial elastic stiffness of the

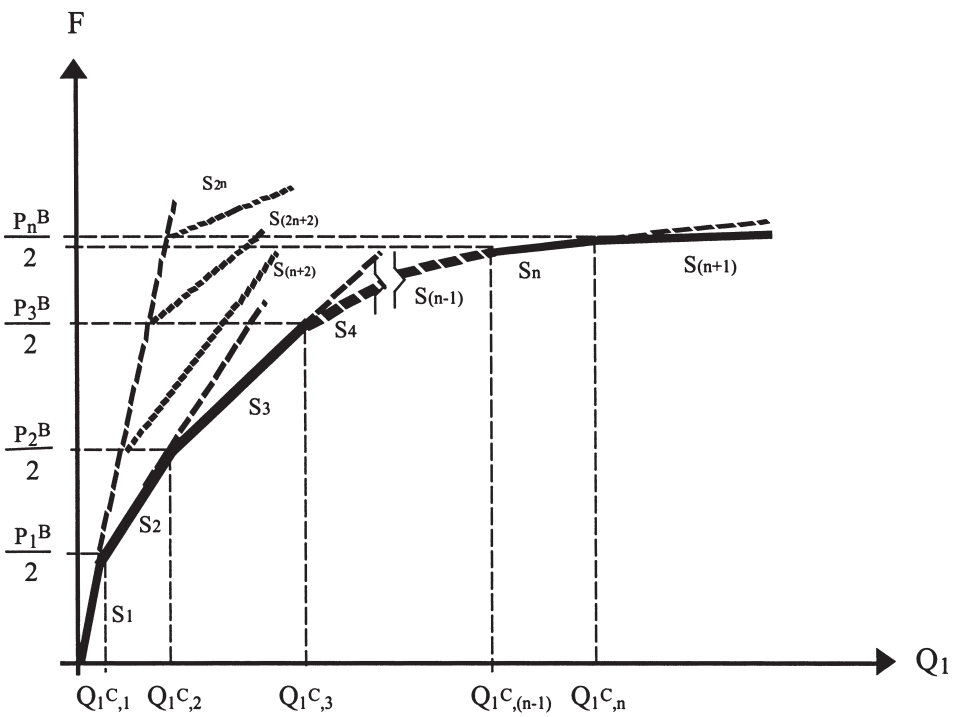

Fig. 7. Typical force-displacement diagram for assembly of springs in series.

assembly of components in series, $k_{p,eq}$ the corresponding post-limit stiffness and P^{B}_{eq} twice the limit force for the equivalent component, using an apropriate transformation criterium, next described:

2.2.1. Transformation criterium 1: equivalent coincident post-buckling stiffness

In this case, both systems yield identical results for the initial stiffness and the *j*th component, the equivalent properties being given by

$$k_{e,eq}=\frac{1}{\sum_{i=1}^{n}\frac{1}{k_{ei}}} \qquad k_{p,eq}=\frac{1}{\sum_{i=1}^{j-1}\frac{1}{k_{pi}}} \qquad P^{B}_{eq}=k_{p,eq}\sum_{i=1}^{j-1}\frac{P^{B}_{i}}{k_{pi}} \tag{5}$$

2.2.2. Transformation criterium 2: equivalent secant post-buckling stiffness

In this case, the equivalent model should exhibit the same elastic stiffness, already derived in Eq. (5), while the equivalent post-limit stiffness should be defined as the straight line between the lowest and the *j*th critical loads, giving

$$k_{e,eq}=\frac{1}{\sum_{i=1}^{n}\frac{1}{k_{ei}}} \qquad k_{p,eq}=\frac{k_{e,eq}m^{(eq.-\mathrm{Crit.2})}}{k_{e,eq}-m^{(eq.-\mathrm{Crit.2})}} \qquad P^{B}_{eq}=P^{B}_{1} \tag{6}$$

where

$$m^{(eq.-\mathrm{Crit.2})}=\frac{P^{B}_{j}-P^{B}_{1}}{(P^{B}_{j}-P^{B}_{1})\sum_{i=1}^{n}\frac{1}{k_{ei}}-\sum_{i=1}^{j-1}\frac{P^{B}_{i}}{k_{pi}}+P^{B}_{j}\sum_{i=1}^{j-1}\frac{1}{k_{pi}}} \tag{7}$$

corresponding P^{B}_{j} to twice the *j*th critical load.

2.2.3. Transformation criterium 3: equivalent lower-bound minimum post-buckling stiffness

Again in this case, the equivalent model should exhibit the same elastic stiffness and the same equivalent pre-compression as the previous case, the equivalent post-limit stiffness being defined from equilibrium solution *n*+1, yielding

$$k_{e,eq}=\frac{1}{\sum_{i=1}^{n}\frac{1}{k_{ei}}} \qquad k_{p,eq}=\frac{1}{\sum_{i=1}^{n}\frac{1}{k_{pi}}} \qquad P^{B}_{eq}=P^{B}_{1} \tag{8}$$

2.3. Equivalent elastic system for elastic-plastic springs in parallel

Analogous to the previous section, it is also required to replace a sequence of components assembled in parallel with a single equivalent spring, as shown in Fig. 8(a). Following [4], the $2n+1$ degree-of-freedom system of Fig. 8(b) is considered, which comprises the following degrees-of-freedom

Q_1 — total displacement at the level of force F;
Q_{1_i} — displacement of elastic spring i;

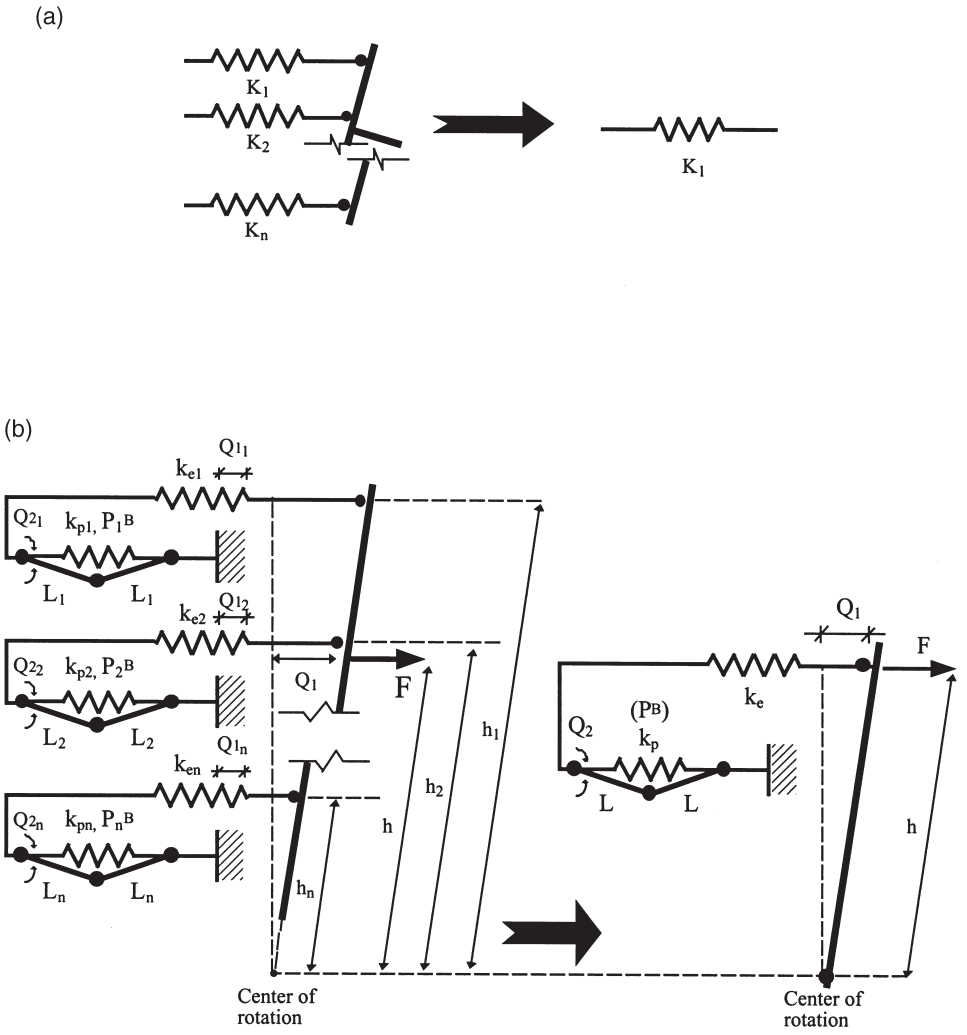

Fig. 8. Equivalent transformation for assembly of components in parallel. (a) Single equivalent elastic-plastic spring; (b) Equivalent elastic system transformation.

Q_{2_i} — rotation of rigid links of length L_i;

yielding the following 2^n equilibrium paths, reproduced from [4] for the particular case of two components in parallel (n=2),

S_1: Fundamental (linear elastic) solution:

$$\begin{cases} Q_{2_1}=0 \\ Q_{2_2}=0 \end{cases} \Rightarrow F=\sum_{i=1}^{2}\frac{h_i^2 k_{ei}}{h^2}Q_1 \tag{9}$$

S_2 to S_3: Uncoupled solutions in each spring:

$$F^{(j+1)}=\left[\frac{h_j^2}{h^2}\frac{1}{\dfrac{1}{k_{ej}}+\dfrac{1}{k_{pj}}}+\frac{h_i^2}{h^2}k_{ei}\right]Q_1+\frac{h_j}{2h}\frac{k_{ej}P_j^{\mathrm{B}}}{k_{ej}+k_{pj}},\ 1\le j\le 2, i\ne j \tag{10}$$

S_4: Fully coupled solution:

$$F=\sum_{i=1}^{2}\frac{h_i^2}{h^2}\frac{1}{\dfrac{1}{k_{ei}}+\dfrac{1}{k_{pi}}}Q_1+\sum_{i=1}^{2}\frac{h_i}{2h}\frac{k_{ei}P_i^{\mathrm{B}}}{k_{ei}+k_{pi}} \tag{11}$$

corresponding to the force-displacement diagram of Fig. 9.

Similarly to the equivalent system for an assembly in series, the equivalent elastic system of Fig. 8(b) is established using an appropriate transformation criterium, yielding the following general expressions for the particular case of three components assembled in parallel, $m^{(j)}$ and $b^{(j)}$ being next defined:

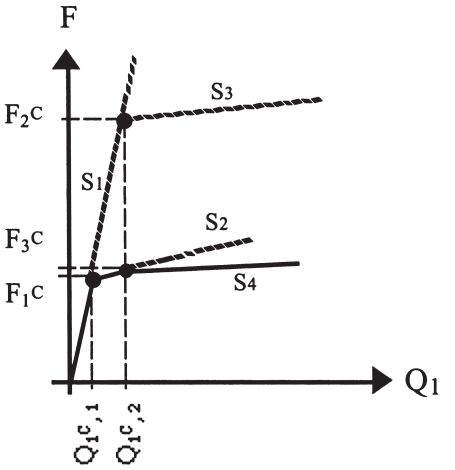

Fig. 9. Typical force-displacement diagram for assembly of springs in parallel.

$$k_{e,eq}=\sum_{i=1}^{2}\frac{h_i^2 k_{ei}}{h^2} \qquad k_{p,eq}=\frac{k_{e,eq}m^{(j)}}{k_{e,eq}-m^{(j)}} \qquad P_{eq}^{B}=2b^{(j)}\frac{k_{e,eq}}{k_{e,eq}-m^{(j)}} \tag{12}$$

2.3.1. Transformation criterium 1: equivalent coincident post-buckling stiffness

Matching the equivalent post-buckling path to equilibrium solution S_2 gives, after [4],

$$m^{(2)}=\frac{h_1^2}{h^2}\frac{1}{\dfrac{1}{k_{e1}}+\dfrac{1}{k_{p1}}}+\frac{h_2^2}{h^2}k_{e2} \qquad b^{(2)}=\frac{h_1}{2h}\frac{k_{e1}P_1^{B}}{k_{e1}+k_{p1}} \tag{13}$$

Alternatively, matching the equivalent post-buckling path to equilibrium solution S_4 gives,

$$m^{(4)}=\sum_{i=1}^{2}\frac{h_i^2}{h^2}\frac{1}{\dfrac{1}{k_{ei}}+\dfrac{1}{k_{pi}}} \qquad b^{(4)}=\sum_{i=1}^{2}\frac{h_i}{2h}\frac{k_{ei}}{k_{ei}+k_{pi}}P_i^{B} \tag{14}$$

2.3.2. Transformation criterium 2: equivalent secant post-buckling stiffness

In this case, the equivalent post-limit stiffness should be defined as the straight line between the lowest and the 3rd critical loads, with

$$m^{(eq.-\mathrm{Crit.2})}=\frac{h_1h_2k_{e1}k_{e2}\left[\dfrac{h_1}{h}\dfrac{k_{e1}}{k_{e1}+k_{p1}}\left(P_1^{B}+\dfrac{h_1k_{p1}}{h_2k_{e2}}P_2^{B}\right)-\dfrac{h_2^2k_{e2}P_1^{B}}{hh_1k_{e1}}+\dfrac{h_2P_2^{B}-h_1P_1^{B}}{h}\right]}{h(h_1k_{e1}P_2^{B}-h_2k_{e2}P_1^{B})} \tag{15}$$

the equivalent pre-compression being written directly as

$$P_{eq}^{B}=\sum_{i=1}^{2}h_i^2k_{ei}\times\frac{P_1^{B}}{2hh_1k_{e1}} \tag{16}$$

2.3.3. Transformation criterium 3: equivalent lower-bound minimum post-buckling stiffness

Again in this case, the equivalent model should exhibit the same elastic stiffness and the same equivalent pre-compression as the previous case, the equivalent post-limit stiffness being defined from equilibrium solution S_4, given by

$$k_{e,eq}=\sum_{i=1}^{2}\frac{h_i^2k_{ei}}{h^2} \quad m^{(eq.-\mathrm{Crit.3})}=m^{(4)}=\sum_{i=1}^{2}\frac{h_i^2}{h^2}\frac{1}{\dfrac{1}{k_{ei}}+\dfrac{1}{k_{pi}}} \quad P_{eq}^{B}=\sum_{i=1}^{2}h_i^2k_{ei}\times\frac{P_1^{B}}{2hh_1k_{e1}} \tag{17}$$

2.4. General non-linear model of a steel connection

Using the equivalent systems derived above, a simplified general model can be proposed that caters for bi-linear component behaviour both in the tensile and compressive zones, illustrated in Fig. 10 for negative (hogging) moment, where q_1 denotes the total rotation of the joint, q_2 and q_3 the rotation of the rigid links, q_4 the axial displacement of the connection and indexes t and c denote, respectively, tension and compression. Introducing, where appropriate, the equivalent properties of Eqs. (5, 6) and (8) for the assemblies in series and Eqs. (12)–(17) for the assemblies in parallel, the following results are obtained [3]:

(i) Fundamental solution

$$\begin{cases} M=\dfrac{z^2 k_{ec}k_{et}}{2(k_{ec}+k_{et})}\sin(2q_1) \\ q_2=0 \\ q_3=0 \end{cases} \tag{18}$$

(ii) Non-linear solution in q_2

$$\begin{cases} M=\dfrac{zk_{ec}k_{et}}{k_{ec}+k_{et}}\left[z\sin q_1-\dfrac{2zk_{ec}k_{et}\sin q_1-P_C^B(k_{ec}+k_{et})}{2[k_{pc}(k_{ec}+k_{et})+k_{ec}k_{et}]}\right]\cos q1 \\ 1-\cos q_2=\dfrac{2zk_{ec}k_{et}\sin q_1-P_C^B(k_{ec}+k_{et})}{4L_c[k_{pc}(k_{ec}+k_{et})+k_{ec}k_{et}]} \\ q_3=0 \end{cases} \tag{19}$$

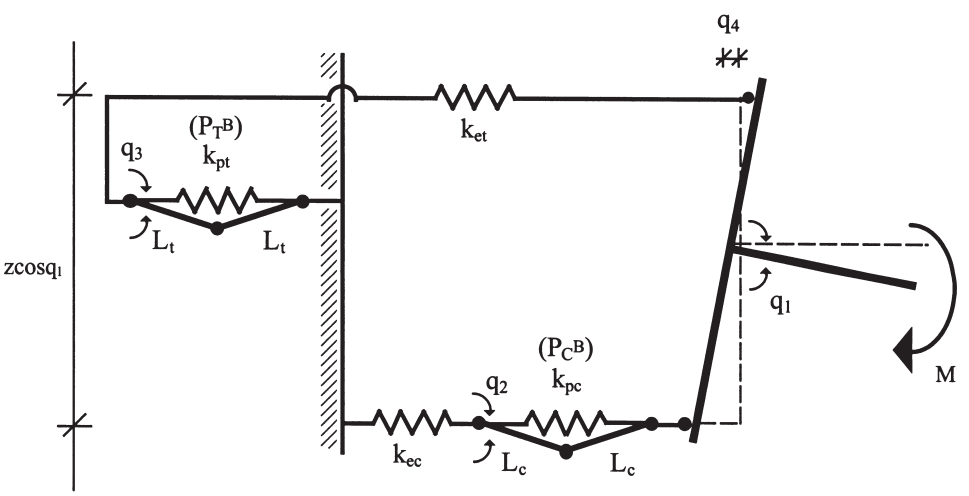

Fig. 10. General equivalent elastic model.

(iii) Non-linear solution in q_3

$$\begin{cases} M=\dfrac{zk_{ec}k_{et}}{k_{ec}+k_{et}}\left[z\sin q_1-\dfrac{2zk_{ec}k_{et}\sin q_1-P_{\mathrm{T}}^{\mathrm{B}}(k_{ec}+k_{et})}{2[k_{pt}(k_{ec}+k_{et})+k_{ec}k_{et}]}\right]\cos q_1 \\ q_2=0 \\ 1-\cos q_3=\dfrac{2zk_{ec}k_{et}\sin q_1-P_{\mathrm{T}}^{\mathrm{B}}(k_{ec}+k_{et})}{4L_{\mathrm{t}}[k_{pt}(k_{ec}+k_{et})+k_{ec}k_{et}]} \end{cases} \tag{20}$$

(iv) Non-linear solution in q_2 and q_3

$$\begin{cases} M=\dfrac{zk_{ec}k_{et}}{k_{ec}+k_{et}}[z\sin q_1-2L_c(1-\cos q_2)-2L_{\mathrm{t}}(1-\cos q_3)]\cos q_1 \\ 1-\cos q_2=\dfrac{2zk_{ec}k_{et}\sin q_1-P_{\mathrm{C}}^{\mathrm{B}}(k_{ec}+k_{et})-4L_{\mathrm{t}}k_{ec}k_{et}(1-\cos q_3)}{4L_{\mathrm{c}}[k_{pc}(k_{ec}+k_{et})+k_{ec}k_{et}]} \\ 1-\cos q_3=\dfrac{2zk_{ec}k_{et}k_{pc}\sin q_1-k_{ec}k_{et}(P_{\mathrm{T}}^{\mathrm{B}}-P_{\mathrm{C}}^{\mathrm{B}})-P_{\mathrm{T}}^{\mathrm{B}}(k_{ec}+k_{et})k_{pc}}{4L_{\mathrm{t}}[k_{ec}k_{et}(k_{pc}+k_{pt})+(k_{ec}+k_{et})k_{pc}k_{pt}]} \end{cases} \tag{21}$$

2.5. Application of transformation procedures

The choice of transformation criteria plays an important role in the evaluation of the moment–rotation response of the connection. For an assembly of components in series (corresponding to bolt row *i*), the equivalence procedure is straightforward since it only depends on the components of bolt row *i*. The chosen equivalence criterium should constitute the best fit to the force-displacement envelope of the components in series.

However, for an assembly of components in parallel, the equivalent transformation depends on the position of the centre of rotation *h* (Fig. 8(b)). Taking the value specified in the revised Annex J of Eurocode 3 [5] as the lever arm *z*,

$$z=\frac{\sum_i k_{eti}z_i^2}{\sum_i k_{eti}z_i} \tag{22}$$

(where *i*: number of bolt rows and z_i: distance between the compression centre of the connection and bolt row *i*), the position of the centre of rotation *h* is obtained using the kinematic compatibility relation that can be established by comparing the models of Fig. 8(b), giving the following equation:

$$\frac{[z_1-(z-h)]^2k_{et1}+[z_2-(z-h)]^2k_{et2}}{h^2}=\frac{z-h}{h}k_{ec} \tag{23}$$

that yields only one meaningful solution for *h* for the range of distances relevant for a steel connection.

Finally, having obtained the moment–rotation response of the connection, it is required to recover the individual results for all components. Since the general model is composed by one equivalent component in the tensile and compressive zones, geometrical compatibility relations yield the axial displacements, Δ^t and Δ^c, for the tensile and compressive zones, taken as positive values, respectively,

$$\Delta^t=\left|q_4-\frac{z}{2}\sin q_1\right| \qquad \Delta^c=q_4+\frac{z}{2}\sin q_1 \tag{24}$$

and the corresponding axial forces, F_t, and F_c:

$$F_c=F_t=\frac{M}{z\cos q_1}. \tag{25}$$

Knowing the total force acting on an equivalent component in series, the displacement of component i is given by

$$\Delta_i=\Delta_{e,i}+\Delta_{p,i} \tag{26}$$

where $\Delta_{e,i}$ denotes the elastic displacement and $\Delta_{p,i}$ the corresponding plastic displacement, given by

$$\Delta_{e,i}=Q_{1_i}=\frac{F}{k_{ei}} \tag{27}$$

and

$$\Delta_{p,i}=\begin{cases}0 \Leftarrow F<\dfrac{P_i^B}{2}\\[2ex] \dfrac{F-\dfrac{P_i^B}{2}}{k_{pi}} \Leftarrow F\geq\dfrac{P_i^B}{2}\end{cases} \tag{28}$$

Analogously, for an assembly of components in parallel, the total displacement of each component is given by

$$\Delta_i=\frac{h_i}{h}\Delta \tag{29}$$

Δ denoting the total displacement at the level of the resultant force F (t or c), obtained from Eq. (24).

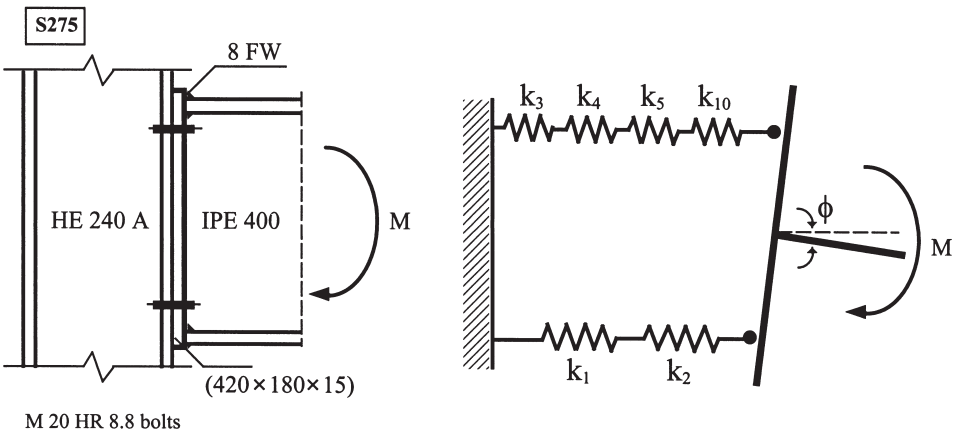

Fig. 11. Bradran 123.001: model of analysis. (a) Connection geometry; (b) Mechanical model.

3. Application to bolted end-plate beam-to-column steel connections

3.1. Flush end-plate bolted beam-to-column connection (Bradran 123.001)

In order to illustrate the application of the equivalent elastic models, one connection configuration was chosen from the literature [6], corresponding to a bolted flush end-plate beam-to-column connection, tested by Bradran at the University of Innsbruck in 1994 and illustrated in Fig. 11(a). In the context of the component method, the spring and rigid link model of Fig. 11(b) is adopted, exhibiting four components in series in the tensile zone, column web in tension (3), column flange in bending (4), end-plate in bending (5) and bolts in tension (10), and two components in the compressive zone, column web in shear (1) and column web in compression (2). Table 1 reproduces the required properties for the various components [2].

Following the procedure defined above and using Eqs. (3) and (4), the minimum envelope for the assemblies in series in the tensile and compressive zones is obtained. Next, adequate choice of the transformation criteria for each case leads to the equiv-

Table 1
Component characterization for flush end-plate beam-to-column connection

Component	Designation	F^C (kN)	k_e (kN/m)	k_p (kN/m)	Δ^y (mm)
Column web in shear	1	327.04	802 220	10 000	0.408
Column web in compression	2	284.79	1 434 300	10	0.199
Column web in tension	3	301.05	1 033 200	10	0.291
Column flange in bending	4	219.47	3 242 400	10 000	0.068
End-plate in bending	5	229.58	3 263 400	10 000	0.070
Bolts in tension	10	282.24	1 663 200	10 000	0.170

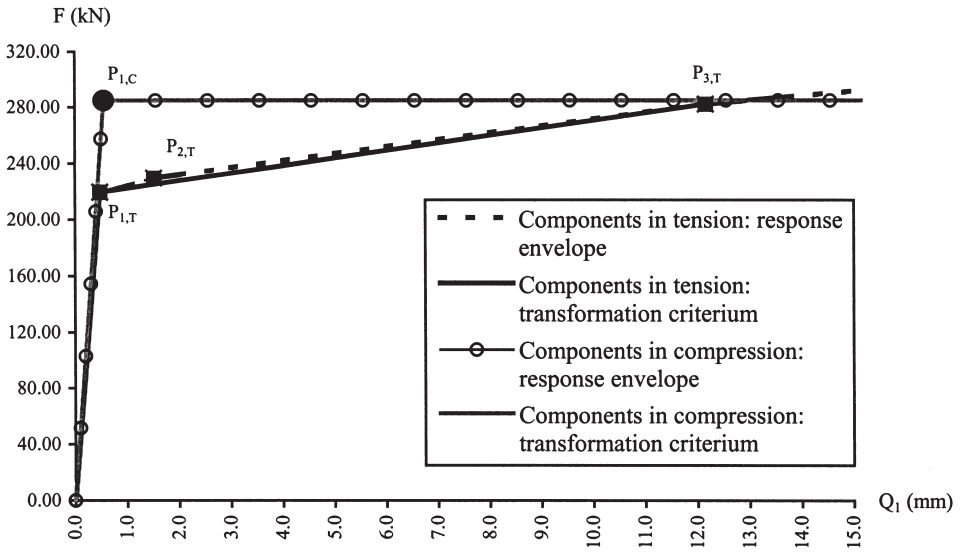

Fig. 12. Bradran 123.001 — Transformation criteria.

alent bi-linear springs, as shown in Fig. 12. It is noted that criterium 1 (equivalent coincident post-buckling stiffness with equilibrium path 2) was chosen for the equivalent compressive spring, while criterium 2 (equivalent secant post-buckling stiffness, joining critical points $P_{1,T}$ and $P_{3,T}$) was chosen for the equivalent tensile spring, since, with reference to Fig. 12, critical point $P_{3,T}$ corresponds to failure of the bolts in tension. The resulting values of the equivalent properties, obtained using Eq. (5) for the compressive spring and Eq. (6) for the tensile spring, are summarized in Table 2. Finally, introducing the equivalent properties in the general model of Fig. 10, using Eqs. (18)–(21), yields the results of Fig. 13.

To assess the accuracy of the present model, these results are compared with the numerical results obtained by Silva et al. [2] and the code predictions of the revised annex J of Eurocode 3 [5]. Fig. 13 shows good correlation between the analytical model and the numerical results, while the Eurocode 3 results, only available for initial stiffness and moment resistance, show differences of about 10%. Since the latter does not provide any quantitative guidance on the evaluation of the ductility of the connection, it will be disregarded in further comparisons. The incremental

Table 2
Equivalent springs for assemblies in series

Equivalent compressive spring	Equivalent tensile spring
k_{ec}=5.145×10^5 kN/m	k_{et}=4.579×10^5 kN/m
k_{pc}=1.000×10^1 kN/m	k_{pt}=5.438×10^3 kN/m
P_C^B=569.58 kN	P_T^B=438.94 kN

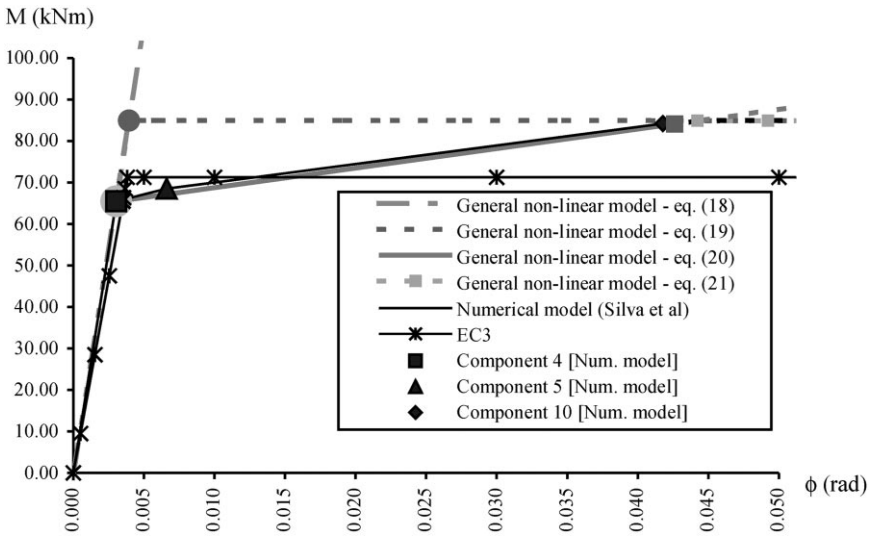

Fig. 13. Bradran 123.001 — Comparative graph.

non-linear analysis performed on the finite element model yields the full moment–rotation response of the connection, allowing, in particular, the identification of the yield points for each component and, consequently, the yielding sequence of the connection: column flange in bending (4), end-plate in bending (5), bolts in tension (10) and, consequently, failure of the connection. The remaning components, column web in shear (1), column web in compression (2) and column web in tension (3), do not yield.

By comparison, the general analytical model, dealing with equivalent components that are restricted to bi-linear behaviour, introduces small errors that are minimised by adequate selection of the transformation criteria, as seen in Fig. 12, where the equivalent post-limit stiffness neglects the bifurcation point $P_{2,T}$. Comparative results for the three procedures are shown in Fig. 13 and summarised in Tables 3 and 4 (values in italic referring to the numerical model). Examination of Table 4 shows the "yield" sequence of the various components and the corresponding levels of ductility: the first component to yield is the column flange in bending, at a yield displacement of 0.068 mm and a total joint rotation of 3.04 mrad (column 3); next, the end-plate in bending reaches yield at 0.070 mm, the total joint rotation reaching

Table 3
Bradran 123.001 — Resistance and initial stiffness

General non-linear model	Numerical model — Silva et al	Eurocode 3
$M_{j.Rd}$=65.5 kNm $S_{j.ini}$=21 550 kN/m	$M_{j.Rd}$=65.5 kNm $S_{j.ini}$=21 359 kN/m	$M_{j.Rd}$=71.2 kNm $S_{j.ini}$=18 659 kN/m

Table 4
Bradran 123.001 — Ductility indexes

Component	Φ_i (Δ_i^f/Δ_i^y)	Component "yield" sequence						Failure
		Absolute displacement Δ_i			Component ductility index			
1	INF	−0.274	−0.286	−0.352	0.671	0.702	0.863	0.863
								0.863
2	5	−0.153	−0.160	−0.197	0.771	0.806	0.991	0.991
								0.991
3	5	0.212	0.222	0.273	0.729	0.763	0.938	0.938
								0.938
4	INF	**0.068**	1.082	6.364	**1.000**	15.982	94.021	**94.021**
		0.068						***93.75***
5	INF	0.067	**0.070**	5.352	0.956	**1.000**	76.090	**76.090**
			0.080					***75.90***
10	1	0.132	0.138	**0.170**	0.778	0.813	**1.000**	**1.000**
				0.170				***1.005***
Joint rotation		Absolute rotation (mrad)		42.62	Joint ductility index		14.032	**14.03**
		3.04	9.44		1.000	3.107		
Bending moment (kNm)		65.46	68.48	84.10				
Joint rotation		*Absolute rotation (mrad)*		*41.78*	*Joint ductility index*		*13.752*	***13.75***
		3.04	*6.61*		*1.000*	*2.177*		
Bending moment (kNm)		*65.47*	*68.50*	*84.18*				

9.44 mrad (column 4); finally, the third component to yield (bolts in tension) and the corresponding values for other components are shown in column 5, with a total joint rotation of 42.62 mrad, that corresponds to the maximum rotation capacity of this connection. It is worth noting that the analytical model is able to recover the individual results for each component using Eqs. (26)–(28), as explained in the previous section. The analytical and numerical solutions show a negligible difference, as seen by evaluating the error in the ductility index [2] of the connection,

$$\varepsilon=\frac{14.03-13.75}{13.75}=0.0204=2.04\% \tag{30}$$

3.2. Extended end-plate bolted beam-to-column connection (Humer 109.003)

To illustrate the transformation procedure for assemblies of components in parallel, a second example was chosen from the literature [6], corresponding to an extended end-plate beam-to-column connection, tested by Humer at the University of Innsbruck in 1987 and shown in Fig. 14(a). Starting with the model of Fig. 14(b), the various component properties are listed in Table 5 [2]. Following a similar procedure to the previous example, the components in series are first transformed, as illustrated in Fig. 15. In this case, criterium 1 (equivalent coincident post-buckling stiffness with equilibrium path 2) was adopted for the equivalent compressive spring, while criterium 2 (equivalent secant post-buckling stiffness, joining critical points $P_{1,T1}$ and $P_{3,T1}$ and critical points $P_{1,T2}$ and $P_{3,T2}$) was chosen for both the first and second rows of the equivalent springs in tension; the resulting equivalent properties are summarized in Table 6.

Next, application of Eqs. (9)–(11) yields the minimum envelope for an assembly

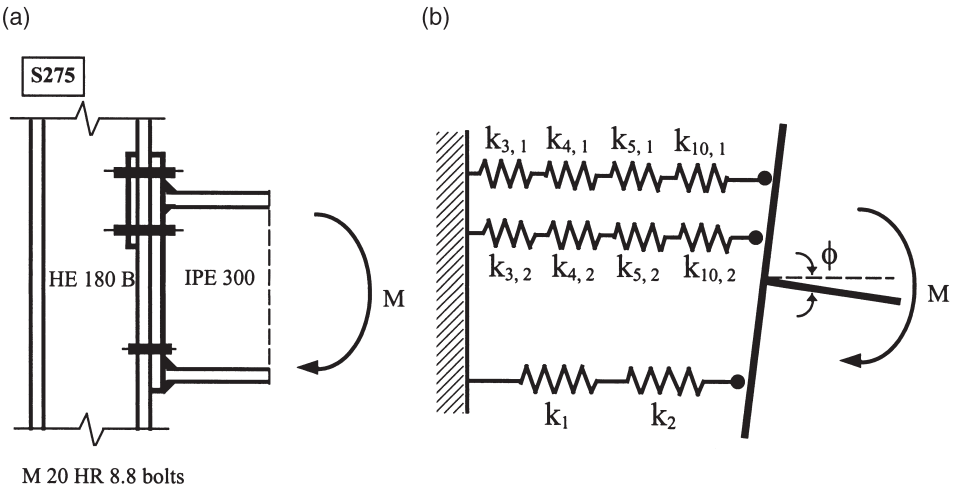

Fig. 14. Humer 109.003: model of analysis. (a) Connection geometry; (b) Mechanical model.

Table 5
Component characterization for extended end-plate beam-to-column connection

Component	Designation	F^C (kN)	k_e (kN/m)	k_p (kN/m)	Δ^y (mm)
Column web in shear	1	262.94	600 600	10 000	0.438
Column web in compression	2	301.30	1 978 200	10	0.152
Column web in tension	3.1	277.29	1 213 800	10	0.228
	3.2	277.29	1 213 800	10	0.228
Column flange in bending	4.1	223.58	2 870 700	10 000	0.078
	4.2	223.58	2 870 700	10 000	0.078
End-plate in bending	5.1	226.70	9 748 200	10 000	0.023
	5.2	267.41	5 859 000	10 000	0.046
Bolts in tension	10.1	282.24	1 789 200	10 000	0.158
	10.2	282.24	1 789 200	10 000	0.158

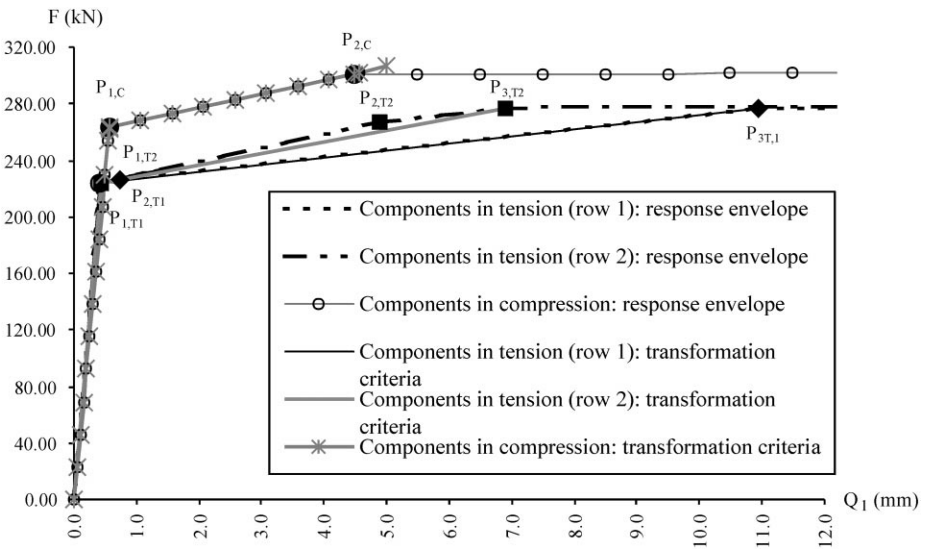

Fig. 15. Humer 109.003 — Transformation criteria (components in series).

Table 6
Equivalent springs for assemblies in series

Equivalent compressive spring	Equivalent tensile spring	
	Bolt row 1	Bolt row 2
k_{ec}=4.607×10^5 kN/m	k_{et1}=5.453×10^5 kN/m	k_{et2}=5.258×10^5 kN/m
k_{pc}=1.000×10^4 kN/m	k_{pt1}=5.150×10^3 kN/m	k_{pt2}=8.446×10^3 kN/m
P_C^B=525.89 kN	P_{T1}^B=447.16 kN	P_{T2}^B=447.16 kN

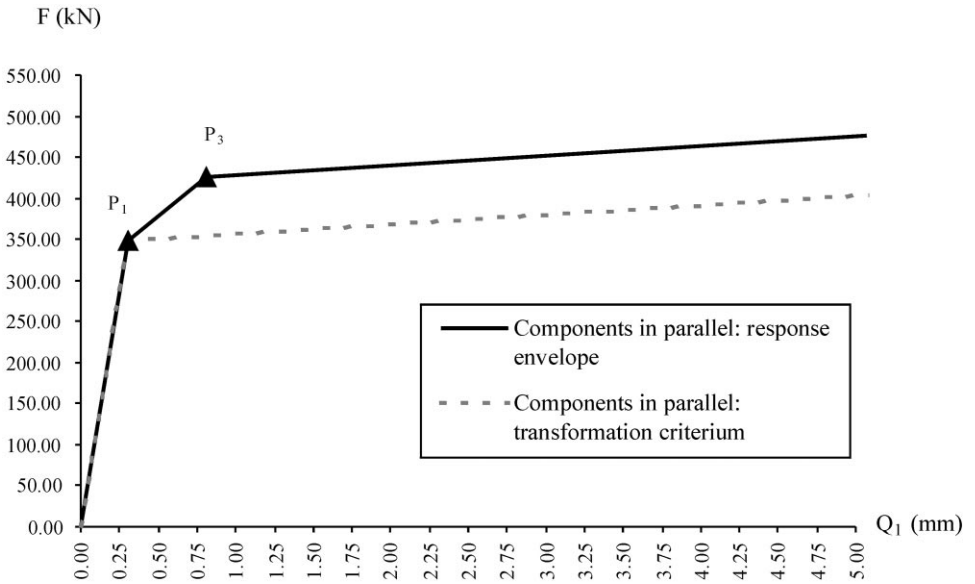

Fig. 16. Humer 109.003 — Transformation criteria (components in parallel).

of two springs in parallel with transformation criterium 3 (equivalent lower-bound minimum post-buckling stiffness) being adopted — Eqs. (12) and (17), giving the resulting bi-linear force-deformation diagram of Fig. 16. Adopting the lever arm given by Eq. (22),

$$z=\frac{k_{et1}z_1^2+k_{et2}z_2^2}{k_{et1}z_1+k_{et2}z_2}=0.2925\text{m} \tag{31}$$

and solving Eq. (23), yields the position of the centre of rotation, h=0.0835 m, and thus the corresponding properties of the equivalent springs for the general non-linear model, shown in Table 7.

Finally, as before, introducing the results of Table 7 in Eqs. (18, 20) and (21) yields the moment–rotation results of Fig. 17. Starting by comparing the moment resistance and initial stiffness obtained analytically with the numerical predictions of Silva et al. [2] and Eurocode 3 [5], good agreement is observed, as shown in Table 8. Similarly, restricting the comparison to the analytical and numerical results,

Table 7
Equivalent springs for assemblies in parallel

Equivalent compressive spring	Equivalent tensile spring
k_{ec}=4.607×10^5 kN/m	k_{et}=1.153×10^6 kN/m
k_{pc}=1.000×10^4 kN/m	k_{pt}=1.183×10^4 kN/m
P_C^B=525.89 kN	P_T^B=694.88 kN

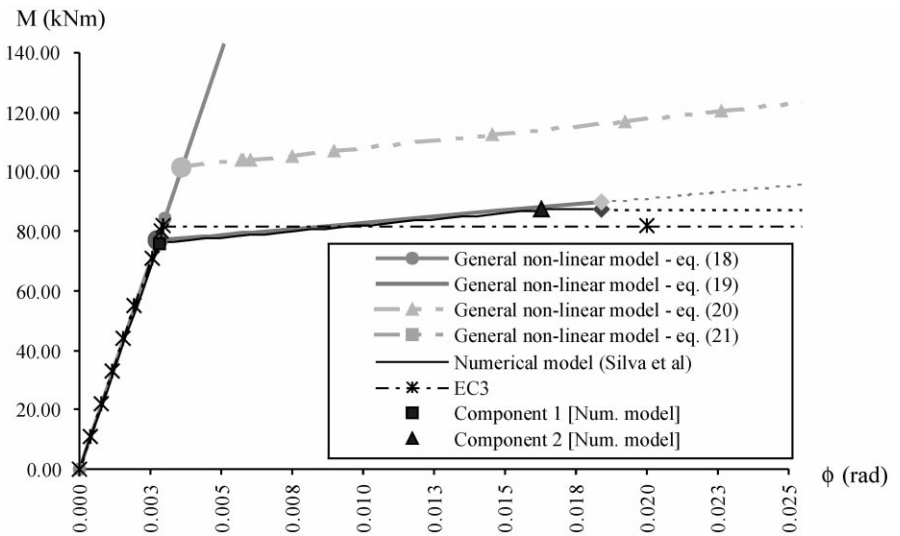

Fig. 17. Humer 109.003 — Comparative graph.

Table 8
Humer 109.003 — Resistance and initial stiffness

General non-linear model	Numerical model — Silva et al	Eurocode 3
$M_{j.Rd}$=**76.9** kNm $S_{j.ini}$=**28 777** kN/m	$M_{j.Rd}$=**76.1** kNm $S_{j.ini}$=**27 005** kN/m	$M_{j.Rd}$=**82.2** kNm $S_{j.ini}$=**26 986** kN/m

it is observed that this connection fails in the compressive zone, the failure sequence corresponding to yielding of the column web in shear (1), yielding of the column web in compression (2) and failure of the column web in compression, for a pre-defined component displacement of five times its yield displacement ($\Delta_2^f=5\Delta_2^y$). In this example, the remaining connection components, column web in tension, column flange in bending, end-plate in bending, and bolts in tension, do not yield before failure. Table 9 and Fig. 17 show good agreement between the analytical and numerical results, as shown by evaluating the relative error in the ductility index of the connection, given by

$$\varepsilon=\frac{6.74-6.52}{6.52}=0.0337=3.37\% \tag{32}$$

Table 9
Humer 109.003 — Ductility indexes

Component	Ψ_i (Δ_i^f/Δ_i^y)	Component "yield" sequence						Failure
		Absolute displacement Δ_i (mm)			Component ductility index			
1	INF	**−0.438**	−4.274	−4.883	**1.000**	9.762	11.154	11.154
		−0.438						*9.763*
2	5	−0.133	**−0.152**	**−0.762**	0.873	**1.000**	**5.000**	5.000
			−0.152	***−0.758***				*5.000*
3.1	5	0.123	0.141	0.144	0.540	0.619	0.632	0.632
								0.577
3.2	5	0.093	0.107	0.109	0.408	0.467	0.477	0.477
								0.525
4.1	INF	0.052	0.060	0.061	0.670	0.768	0.783	0.783
								0.697
4.2	INF	0.039	0.045	0.046	0.506	0.580	0.591	0.591
								0.635
5.1	INF	0.015	0.018	0.018	0.661	0.757	0.773	0.773
								0.707
5.2	INF	0.019	0.022	0.023	0.423	0.485	0.495	0.495
								0.529
10.1	1	0.084	0.096	0.098	0.531	0.608	0.621	0.621
								0.555
10.2	1	0.084	0.072	0.074	0.531	0.459	0.469	0.469
								0.505
Joint rotation		Absolute rotation (mrad)		18.41	Joint ductility index		6.739	***6.74***
		2.73	16.59		1.000	6.073		
Bending moment (kNm)		76.92	88.13	89.92				
Joint rotation		*Absolute rotation (mrad)*		*18.37*	*Joint ductility index*		*6.519*	***6.52***
		2.82	*16.27*		*1.000*	*5.775*		
Bending moment (kNm)		*76.06*	*87.17*	*87.17*				

4. Concluding remarks

The evaluation of the maximum available rotation of a steel connection, essential to enable the safe utilisation of partial-resistant joints in steel construction, is currently not covered by the code specifications of Eurocode 3. There is a consensual opinion in the literature [7] that any general approach to deal with this problem requires characterisation of the various connection components that extends well into the non-linear range, in opposition to the currently available procedures that simply evaluate the component resistance and initial stiffness (the limit force and initial elastic stiffness of Fig. 1).

A recent attempt by Aribert et al. [8] to evaluate the moment–rotation response of a flush end-plate connection using an appropriate component model required an incremental non-linear numerical analysis. The proposed model presents closed-form analytical solutions that, for a given characterisation of the various components, yield the full moment–rotation response of any steel connection loaded in bending currently covered by the revised annex J of Eurocode 3 [5]. It is thus easily translatable into code recommendations with little extra work from the current revised Annex J specifications, with the added advantage of incorporating all required connection properties (resistance, stiffness and ductility) into one single consistent model.

Practical utilisation of this methodology (as, incidentally, any alternative methodology that attempts to predict the non-linear moment–rotation response of a steel connection in the framework of the component method) requires proper characterisation of the non-linear response of each component up to failure, with thorough evaluation of the post-limit stiffness (positive or negative). Given that this task is currently being actively pursued in various european research centres, it is anticipated that this data will become available in the near future, altough some initial results are already available for the component “column web in compression”, that exibits negative post-limit stiffness [9]. Since this model is able to reproduce any non-linear moment–rotation configuration up to failure, comparison with experimental (illustrated in [3] for the simple case of a welded connection) or theoretical (finite element or other) results only depends on adequate characterisation of the components.

Finally, this methodology combined with the component ductility classes and ductility indexes already proposed [2] may lead to simple, deemed-to-satisfy criteria on ductility requirements.

Acknowledgements

Financial support from “Ministério da Ciência e Tecnologia” — PRAXIS XXI research project PRAXIS/P/ECM/13153/1998 and PRODEP II (Sub-programa 1) is acknowledged.

References

[1] Weynand K, Jaspart J-P, Steenhuis M. The stiffness model of revised Annex J of Eurocode 3. In: Bjorhovde R, Colson A, Zandonini R, editors. Connections in Steel Structures III. Proceedings of the 3rd International Workshop on Connections. Italy: Trento, 1995. p.441–52.
[2] Simões da Silva LAP, Santiago A, Vila Real P. Ductility of steel connections. Can J Civil Engng, submitted for publication.
[3] Simões Da Silva LAP, Girão Coelho A, Neto EL. Equivalent post-buckling models for the flexural behaviour of steel connections. Comput Struct 2000;77(6):615–24.
[4] Simões da Silva LAP, Girão Coelho A. Transformation criteria for assemblies of components in series and parallel in steel and composite connections. Solids & Struct, submitted for publication.
[5] Eurocode 3, ENV — 1993-1-1:1992/A2, Annex J, Design of Steel Structures — Joints in Building Frames. CEN, European Committee for Standardization, Document CEN/TC 250/SC 3, Brussels, 1998.
[6] Cruz PJS, Simões Da Silva LAP, Rodrigues DS, Simões RAD. Database for the semi-rigid behaviour of beam-to-column connections in seismic regions. J Constr Steel Res 1998;46:233–4.
[7] Kulhmann U, Davison JB, Kattner M. Structural systems and rotation capacity. COST Conference, Liège, Belgium, 18–19 September 1998.
[8] Aribert JM, Lachal A, Dinga ON. Modélisation du comportement d'assemblages métalliques semi-rigides de type poutre-poteau boulonnés par platine d'extrémité. Const Métallique 1999;1:25–46.
[9] Kulhmann U. Influence of axial forces on the component web under compression. COST-C1 — Working Group Meeting, Thessaloniki, 28 May, C1/WD2/99-01, 1998.